Chem

CellPress

Article

Toward an Integrated Conversion of 5-Hydroxymethylfurfural and Ethylene for the Production of Renewable *p*-Xylene

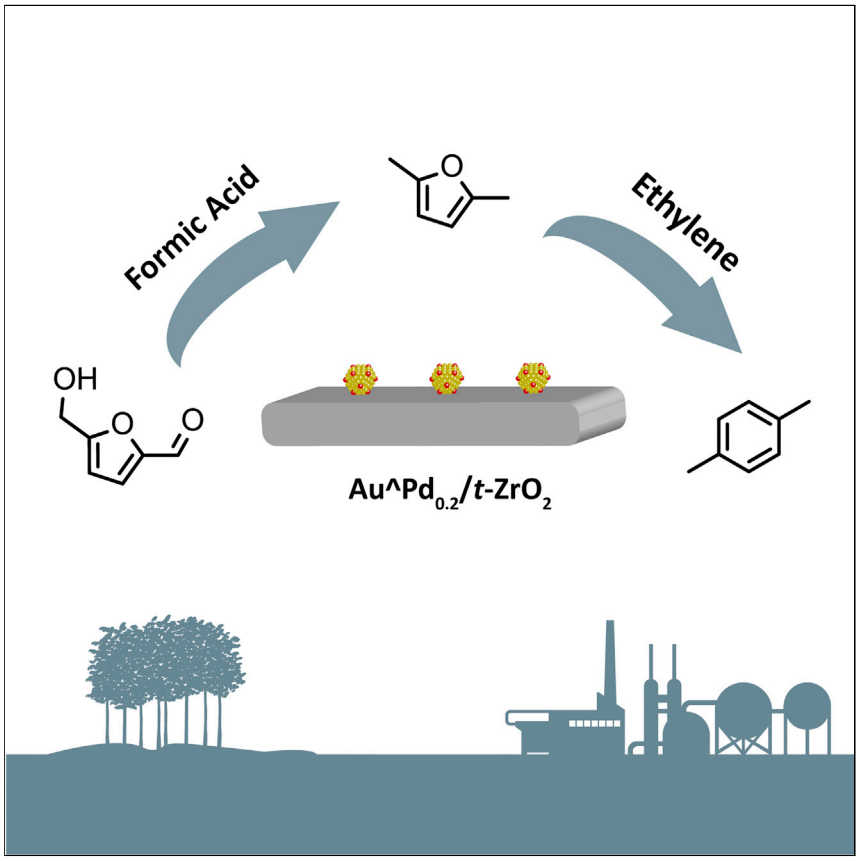

Cao and colleagues describe an alternative strategy for producing *para*-xylene through a more sustainable method than the current bio-based approaches. The strategy relies on an integrated conversion of 5-hydroxymethylfurfural with formic acid and ethylene, made possible by the use of a single multifunctional catalyst based on bimetallic Pd-decorated Au deposited on tetragonal-phase zirconia. The proposed process is particularly appealing because it is fully fossil independent, implying a viable and greener biorefinery scheme.

Lei Tao, Tian-Hao Yan, Wenqin Li, ..., Zhen-Hua Li, He-Yong He, Yong Cao

lizhenhua@fudan.edu.cn (Z.-H.L.)
yongcao@fudan.edu.cn (Y.C.)

HIGHLIGHTS

The direct preparation of *para*-xylene from 5-hydroxymethylfurfural is achievable

A multifunctional Pd-Au-based catalyst displays high selectivity toward *para*-xylene

The superiority of *t*-ZrO_2 as a versatile catalyst support stands out clearly

Tao et al., Chem 4, 1–16
September 13, 2018
https://doi.org/10.1016/j.chempr.2018.07.007

Please cite this article in press as: Tao et al., Toward an Integrated Conversion of 5-Hydroxymethylfurfural and Ethylene for the Production of Renewable *p*-Xylene, Chem (2018), https://doi.org/10.1016/j.chempr.2018.07.007

Chem

CellPress

Article

Toward an Integrated Conversion of 5-Hydroxymethylfurfural and Ethylene for the Production of Renewable *p*-Xylene

Lei Tao,[1] Tian-Hao Yan,[1] Wenqin Li,[2] Yi Zhao,[1] Qi Zhang,[1] Yong-Mei Liu,[1] Mark M. Wright,[2,3] Zhen-Hua Li,[1,*] He-Yong He,[1] and Yong Cao[1,4,*]

SUMMARY

The use of biomass as a solution to satisfy the pressing needs for a fully sustainable biocommodity industry has been explored for a long time. However, limited success has been obtained. In this study, a highly effective two-stage procedure for the direct preparation of *para*-xylene (PX) from 5-hydroxymethylfurfural (HMF) and formic acid in one pot is described; these chemicals are two of the major bio-based feedstocks that offer the potential to address urgent needs for the green, sustainable production of drop-in chemical entities. The use of a robust, efficient heterogeneous catalyst, namely, bimetallic Pd-decorated Au clusters anchored on tetragonal-phase zirconia, is crucial to the success of this strategy. This multifunctional catalytic system can not only facilitate a low-energy-barrier H_2-free pathway for the rapid, nearly exclusive formation of 2,5-dimethylfuran (DMF) from HMF but also enable the subsequent ultraselective production of PX by the dehydrative aromatization of the resultant DMF with ethylene.

INTRODUCTION

Para-xylene (PX; 1,4-dimethlybenzene) is one of the major commodity chemicals serving a vast range of industries with large global economic impact.[1] Currently the global production of PX amounts to nearly 40 million tons per year,[2] and the majority of PX is produced via distillative extraction of the BTX (benzene, toluene xylene)-rich aromatic fractions from naphtha reforming processes.[3,4] To expand the source of PX production and alleviate excessive reliance on existing petroleum processes, alternative routes to PX production from biorenewable feedstocks have been explored.[5] In this regard, the conversion of 5-hydroxymethylfurfural (HMF), a highly versatile biomass-derived platform molecule, to PX is considered one of the most promising, sustainable, and inherently selective approaches.[6–8] In this sequence, HMF was deoxygenatively transformed to 2,5-dimethylfuran (DMF) that was upgraded with ethylene to PX through a tandem Diels-Alder/dehydration pathway. As opposed to most other related procedures suffering from very poor PX-targeting selectivity,[9–11] this HMF-based procedure holds promise to afford PX as the sole product and is of great industrial potential, especially when an efficient and practical catalytic system can be employed (Scheme 1). With recent advances in biorefinery technologies enabling cost-effective, highest-volume production of HMF from abundantly available lignocellulosic biomass,[12–16] the HMF-to-PX process is expected to become increasingly competitive for future PX manufacturing.

The Bigger Picture

With increasing pressure around the world to move toward a bio-based economy, it is essential that industrially important commodity chemicals can be readily accessed from biomass resources. *Para*-xylene (PX) synthesis is one such target that is being actively pursued through the development of several biorefinery schemes based on integrated biomass processing. Significant progress has recently been achieved either in the selective synthesis of biorenewable PX from Diels-Alder-like coupling of ethylene with 2,5-dimethylfuran (DMF) or making DMF from 5-hydroxymethylfurfural (HMF) using hydrogen as the terminal reductant. However, a green and direct conversion of HMF, an essential feedstock source for future biorefinery schemes, into PX has yet to be developed. We have established an integrated process that directly converts HMF to PX in a highly compact and hydrogen-independent manner, thereby providing a new perspective on the potential of advanced biorefinery technologies.

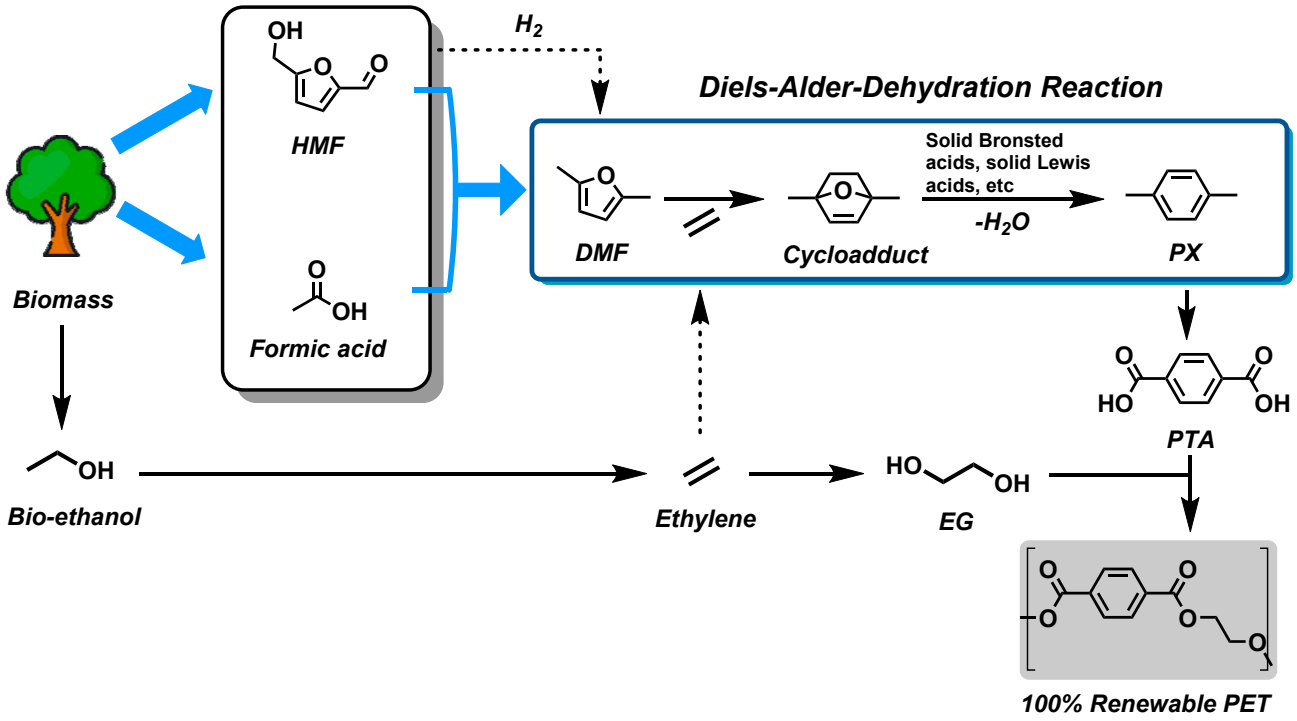

Scheme 1. On-Purpose Synthesis of PX Starting from Renewable HMF

The key to the success of HMF-to-PX conversion is to develop highly advanced and versatile catalytic systems that can achieve high levels of target PX selectivity. Because of the inherent complexity of the reaction pathways associated with the required tandem Diels-Alder/dehydration sequence,[17,18] a robust and durable solid acid catalyst enabling direct PX production from DMF with sufficient selectivity has yet to be developed. Even more challenging is the development of an efficient and affordable catalytic system for the reductive conversion of HMF to DMF in a highly selective and H_2-independent manner.[19–24] Given that fossil-based H_2 is currently deemed as a less-favored part of the biorefinery concept, minimizing or eliminating H_2 utilization has become essential in the context of sustainable production processes based on bioderivable feedstocks.[25,26] Formic acid (FA), an emerging reversible hydrogen storage material by virtue of its inherently biorenewable nature and high gravimetric energy density,[27–29] is particularly appealing in this regard,[19–21] offering unique opportunities to develop alternative reductive procedures capable of achieving a higher level of selectivity control.[30–33] Despite the anticipated benefits of using FA for making DMF from HMF, a suitable catalyst that is sufficiently potent for such a transformation still remains elusive.

To the best of our knowledge, a straightforward and one-pot procedure capable of directing the H_2-free formation of PX starting from HMF has not been reported. This challenging goal would be of clear significance and interest, especially if the overall process can be realized using only one single solid catalyst system. Herein, we report such a potent catalyst system that can enable ultraselective production of PX starting directly from HMF. More specifically, we show that Pd-decorated Au (Au^Pd) nanoparticles (NPs) anchored on amphoteric zirconia is a robust dual catalyst that combines the excellent performance for H_2-independent hydrogenolysis of HMF to DMF related to the Pd-decorated Au sites with the high selectivity for subsequent

[1]Shanghai Key Laboratory of Molecular Catalysis and Innovative Materials, Department of Chemistry, Fudan University, Shanghai 200433, China

[2]Department of Mechanical Engineering, Iowa State University, Ames, IA 50011, USA

[3]Bioeconomy Institute, Iowa State University, Ames, IA 50011, USA

[4]Lead Contact

*Correspondence: lizhenhua@fudan.edu.cn (Z.-H.L.), yongcao@fudan.edu.cn (Y.C.)

https://doi.org/10.1016/j.chempr.2018.07.007

Please cite this article in press as: Tao et al., Toward an Integrated Conversion of 5-Hydroxymethylfurfural and Ethylene for the Production of Renewable *p*-Xylene, Chem (2018), https://doi.org/10.1016/j.chempr.2018.07.007

PX production from DMF and ethylene associated with the underlying support. Moreover, we show that it is possible to integrate the Au^Pd-catalyzed HMF-to-DMF reaction, which can be favorably accomplished by employing biogenic FA as a convenient, versatile, and safe hydrogen source and the crucial dehydrative DMF-ethylene cycloaddition into a one-pot catalytic process.

RESULTS

Catalyst Development for HMF to DMF

At the outset of our work, we sought to identify a superior catalyst that can enable a facile HMF-to-DMF conversion by using FA as the sole reducing reagent. A recent report by Rauchfuss and co-workers for deoxygenative conversion of HMF to DMF with FA using a commercial Pd/C catalyst attracted our attention.[34] In our case, however, attempts to apply Rauchfuss's protocol to HMF-to-DMF conversion did not prove efficacious, underscoring the need for exploring alternative catalytic systems. Building upon our recent findings concerning the unusual capability of heterogeneous gold-based catalysts for FA activation and related processes,[30–33] we initiated our investigation by examining a series of monometallic Au-based catalysts comprising Au NPs (average size <3 nm) deposited on various inorganic oxide supports (Figure S1). Initial testing was conducted under the conditions of 140°C, 0.1 MPa N_2, and 1:10 mixture of HMF/FA in 1,4-dioxane using a catalyst loading of 0.4 mol %. As often reported for gold-based catalysts,[30–32] we anticipated that the nature of the underlying support materials would play a vital role for success. As shown in Table 1, this was indeed the case: while gold on single tetragonal-phase zirconia (*t*-ZrO_2) provided promising results for DMF formation from HMF (Table 1, entry 1), the use of other related supports was rather unsatisfactory (Table 1, entries 2–6).

It is worth mentioning that the desired FA-mediated deoxygenation was not accomplished with other noble metal catalysts, such as Pt, Pd, or Ru deposited on *t*-ZrO_2 (Table S1, entries 1–3)—a strong testament to the unique potential of mild Au catalysis. We posited that the failure of the platinum-group metal (PGM)-based catalysts was due to the lack of adequate capability to enable dehydrogenative activation of FA. In fact, the results from detailed reaction monitoring of these catalysts indicate only traces of reduced derivatives of HMF, with the formate ester being invariably identified as the only product (Table S1). This observation supports the view that catalysts based on individual PGMs are incapable of activating FA under present conditions and that a suitably prepared gold catalyst can facilitate FA activation in an efficient and highly desired manner. This is further confirmed by a separate set of experiments involving FA as the sole reactant; as shown in Figure S2, FA decomposition on the catalyst Au/*t*-ZrO_2 in 1,4-dioxane produces H_2 much more efficiently than its PGM-based counterparts, as well as the corresponding systems comprising gold deposited on other supports. All these results clearly demonstrate that, in the present system, the combination of gold and *t*-ZrO_2 plays a pivotal role in favoring DMF formation during the FA-mediated HMF conversion.

In the course of optimizing the different process parameters, attempts to improve the DMF yield by varying the reaction temperature and solvent (Table S2), as well as altering the gold content in the Au-*t*-ZrO_2-based systems (Table S1, entries 8, 9), were unsuccessful. Considering that bimetallicity promises widely tunable catalytic properties, we turned our attention to the combination of Au NPs with a second metal from PGMs. This was achieved by subjecting preformed Au/*t*-ZrO_2 obtained by deposition-precipitation to a $NaBH_4$-mediated reductive treatment in the presence of a metal salt precursor of Pd, Pt, or Ru (denoted as Au^M_x/*t*-ZrO_2;

Please cite this article in press as: Tao et al., Toward an Integrated Conversion of 5-Hydroxymethylfurfural and Ethylene for the Production of Renewable *p*-Xylene, Chem (2018), https://doi.org/10.1016/j.chempr.2018.07.007

Table 1. FA-Mediated Catalytic Conversion of HMF into DMF Using Various Catalysts

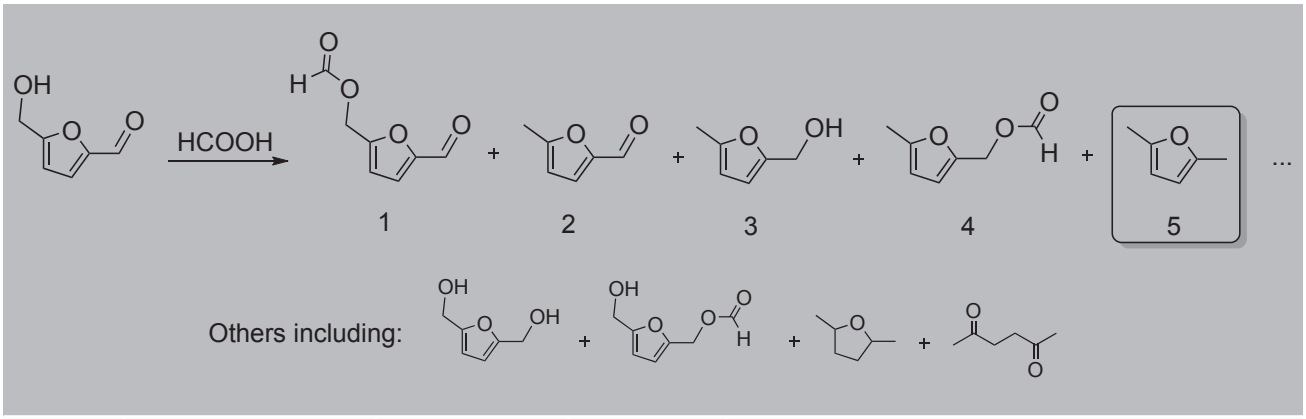

Entry	Catalyst	Metal (mol %)	Conv. (%)	Yield (%)					
				1	2	3	4	5	Others
1	1% Au/*t*-ZrO_2	0.4	99	12	10	2	2	70	3
2	1% Au/*m*-ZrO_2	0.4	99	54	15	–	1	23	6
3	1% Au/TiO_2	0.4	>99	9	12	2	–	61	16
4	1% Au/Al_2O_3	0.4	72	52	8	–	1	6	5
5	1% Au/CeO_2	0.4	78	58	10	–	–	8	2
6	1% Au/SiO_2	0.4	79	79	–	–	–	–	–
7	1% Au^$Pd_{0.05}$/*t*-ZrO_2	0.4	>99	–	–	2	–	97	1
8	1% Au^$Pt_{0.05}$/*t*-ZrO_2	0.4	89	36	13	–	1	34	5
9	1% Au^$Ru_{0.05}$/*t*-ZrO_2	0.4	94	24	13	2	1	43	11
10	1% Au^$Pd_{0.05}$/*t*-ZrO_2	0.25	91	25	17	2	1	43	3
11	1% Au^$Pd_{0.1}$/*t*-ZrO_2	0.25	>99	1	4	6	2	85	2
12	1% Au^$Pd_{0.2}$/*t*-ZrO_2	0.25	>99	–	–	1	–	98	1
13	1% Au^$Pd_{0.5}$/*t*-ZrO_2	0.25	99	30	15	2	2	47	3

Reaction conditions: 2 mmol HMF, 20 mmol FA, 0.1 MPa N_2, 5 mL 1,4-dioxane, 140°C, 1.5 hr; and the catalyst is indicated in column 2.

for details, see Supplemental Information). Analysis by transmission electron microscopy (TEM) revealed that the sizes of the particulate matter were essentially identical in both the Au/*t*-ZrO_2 and the resultant bimetallic materials, inferring a preferential deposition of the PGM species onto the Au surface (Figure S3). Notably, this is accompanied by a prominent modification of the electronic properties of the Au particles, as revealed by X-ray photoelectron spectroscopy (XPS) measurements (Figure S4). Much to our delight, Au^$Pd_{0.05}$/*t*-ZrO_2 with a Pd/Au molar ratio of 1:20 showed a dramatic bimetallic promotion of DMF synthesis in HMF conversion. With this catalyst, it was possible to achieve an excellent selectivity toward DMF, which was obtained in 97% yield after only 1.5 hr at 140°C (Table 1, entry 7).

Spurred by these results, we sought to assess the efficacy of a series of *t*-ZrO_2-supported Au-Pd bimetallic catalysts with the same chemical composition as the Au^$Pd_{0.05}$/*t*-ZrO_2 material but featuring different binary mixing levels and various degrees of structural uniformity. The preparation procedure for these Au-Pd/*t*-ZrO_2 bimetallic catalysts and relevant characterization data are provided in Supplemental Information. These catalysts, however, were not found to be particularly effective, although in all cases very high to total conversion of HMF can be readily attained (Table S3). It should be noted that a similarly constituted reference catalyst

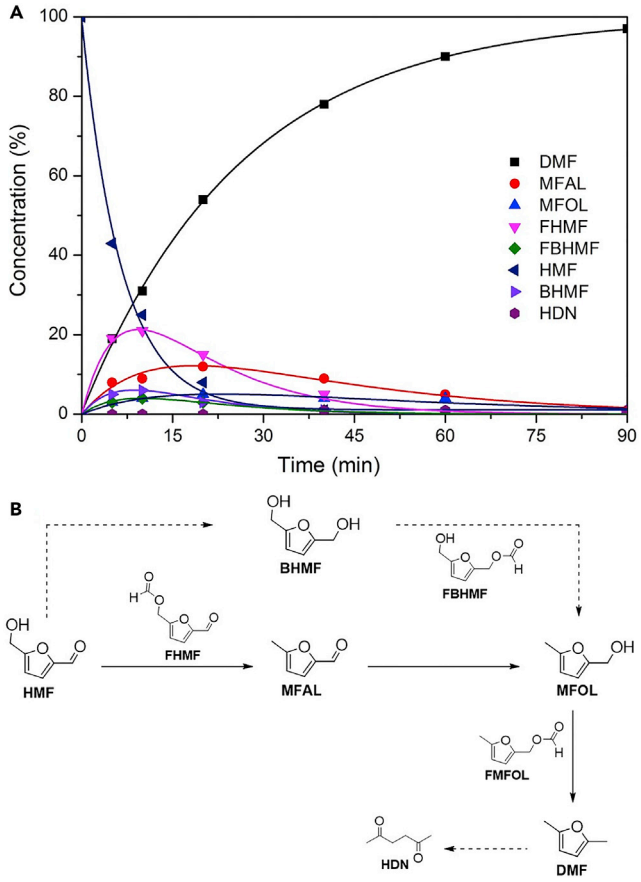

Figure 1. Reaction Progress of FA-Mediated HMF C onversion to DMF

(A) Time-course plot.

(B) Reaction network for FA-mediated HMF conversion to DMF.

Reaction conditions: 2 mmol HMF, 20 mmol FA, 0.4 mol % Au^$Pd_{0.05}$/*t*-ZrO_2, 0.1 MPa N_2, 5 mL 1,4-dioxane, 140°C, 1.5 hr.

comprising *t*-ZrO_2-supported uniform Au-Pd bimetallic alloy NPs, which has been carefully prepared by a colloidal deposition approach with benchmark characteristics (see Figure S5 for characterization details), has also been proved to display inferior performance in terms of target-specific DMF formation, despite the reported advantages of Au-Pd-based alloy formulations for a variety of organic transformations including direct synthesis of hydrogen peroxide, selective alcohol oxidation, and selective oxidation of carbon-hydrogen bonds.[35–37] These results underscore the critical importance of controlling both the structural and chemical nature of the Pd/Au/*t*-ZrO_2 interfaces for the desired catalysis.

Interestingly, with the replacement of the FA by H_2 in the reaction, the expected DMF formation barely occurred under otherwise identical conditions using Au^$Pd_{0.05}$/*t*-ZrO_2 as the catalyst, with 2,5-bishydroxymethylfuran (BHMF) obtained as the primary product (Table S4, entry 1). In fact, a significantly higher temperature (greater than 220°C) is required to facilitate appreciable formation of DMF under H_2 (Table S4, entry 2; Figure S6). These observations, along with the fact that the FA-mediated conversion of HMF proceeds via multiple deoxygenation events involving the formation of formate ester derivatives of HMF and 5-methylfurfuryl alcohol (MFOL) as intermediates in the production of DMF (Figure 1), demonstrated the

Please cite this article in press as: Tao et al., Toward an Integrated Conversion of 5-Hydroxymethylfurfural and Ethylene for the Production of Renewable *p*-Xylene, Chem (2018), https://doi.org/10.1016/j.chempr.2018.07.007

crucial role of FA in considerably decreasing the energy barrier for DMF formation, presumably because of the creation of a kinetically more favorable pathway associated with the deoxygenation of formate species. This is clearly the decisive factor in promoting a desirable low-temperature C-O cleavage in HMF molecules. To confirm that FA-related intermediates exert a positive effect on the promotion of the crucial C-O scission, we subjected both MFOL and its corresponding formate ester to hydrogenative reaction at 140°C (Figure S7). Upon the reaction conducted with 5-methylfururfylformate (FMFOL), the DMF formation rate dramatically increased. This finding, along with the fact that the activation energy for DMF formation directly from MFOL is 14.5 $kJ \cdot mol^{-1}$ greater than that from MFOL via FMFOL (Figure S8), substantiates the unique capability imparted by FA to create an efficient formylation-decarboxylative deoxygenation (FDDO) pathway with an exceptionally low energy barrier.

The prominent role of FA in enabling the facile formation of DMF under energy-efficient conditions is further emphasized by the fact that a significantly higher overall yield of DMF was achieved using an additional 5 equiv of FA for H_2-assisted HMF reduction under otherwise identical conditions (Table S5, entries 1 and 2). Notably, although FA is an important contributing factor for facilitating the generation of DMF, the use of 5 equiv of only FA is not sufficient to convert HMF to high amounts of DMF, which is reflected in the rather low yield observed in entry 1, where other than 5-methylfurfural (MFAL) and MFOL, significant amounts of DMF were not obtained during the reaction. This observation, coupled with the fact that only the use of 15 equiv of FA can lead to the formation of an appreciable amount of 2,5-methyltetrahydrofuran as a result of the over-reduction of the furan ring (Table S5, entry 4), indicates that the intricate control over the interplay between the FA-mediated hydrogenation and hydrogenolysis pathways using a $Au^Pd_{0.05}/t\text{-}ZrO_2$ catalyst is crucial to achieving the desired outcome. To gain additional mechanistic insight into the molecular events that are crucial for DMF formation, we also subjected possible intermediates as inferred from Figure 1 to the FA-mediated reaction under the optimized reaction conditions. As summarized in Table S6, the rates for transformation of formyl-5-hydroxymethylfurfural (FHMF) to MFAL and FMOL to DMF were consistently slower than those of the other three steps, suggesting the rate-determining nature of the decarboxylation steps.

Collectively, these observations indicate a critical and multifaceted role of FA in enabling the facile conversion of HMF to DMF, first as the hydrogen source and second as the FDDO reagent for oxygen removal. The specific rates for the decomposition of FA alone and the sole decarboxylation of FMFOL occurred much faster over $Au^Pd_{0.05}/t\text{-}ZrO_2$ than any other materials tested (Figures S9A and S9B), which further supports the proposed multifaceted role of FA. To better understand the physicochemical characteristics of the bimetallic $Au^Pd_x/t\text{-}ZrO_2$ system, while simultaneously improving its catalytic behavior, we prepared three additional $Au^Pd_x/t\text{-}ZrO_2$ catalysts with different molar ratios of Pd/Au and evaluated them at a catalyst loading level far lower than 0.4 mol %. Intriguingly, this has proved to be particularly beneficial for further optimizing the FDDO capability of these bimetallic Au-based catalysts (Figures S9C and S9D). From the results obtained by XPS, the electronic state of metallic Au clusters in all of these samples (Figure S10) was clearly affected by the addition of Pd, indicating a distinct electronic promoting effect of Pd (albeit in very small amounts) with respect to the crucial $Au/t\text{-}ZrO_2$-catalyzed FDDO process. This scenario is further supported by infrared studies of CO adsorption (Figure S11): bands corresponding to linearly adsorbed CO, related to negatively charged Au edge sites and bridging CO adsorbed on surface-decorated Pd species, which were predominantly located on the surface of the original Au corner sites,[38,39] were observed.

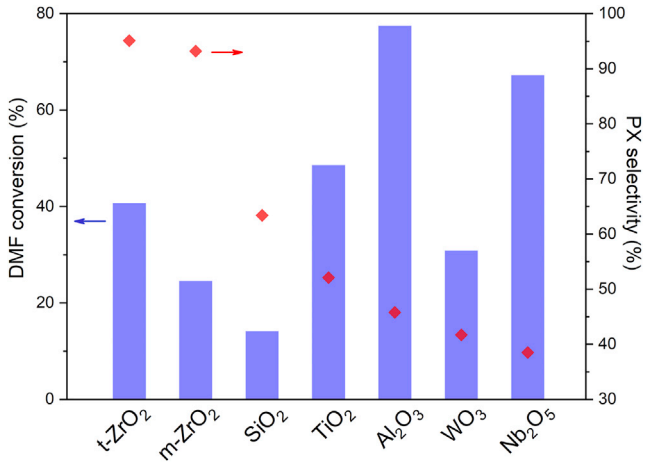

Figure 2. Dehydrative Aromatization of DMF with Ethylene for PX Synthesis Using Various Metal Oxides

Reaction conditions: 1 mmol DMF, 4 MPa ethylene, 5 mL *n*-heptane, 300 mg catalyst, 250°C, 6 hr.

Eventually, the Au^$Pd_{0.2}$/*t*-ZrO_2 catalyst with a Pd/Au molar ratio of 1:5, exhibiting the highest FDDO efficiency, afforded DMF in an essentially quantitative yield (ca. 98%) at an extremely low catalyst loading of 0.25 mol % (Table 1, entry 12). In this specific case, the average turnover frequency (TOF) reached as high as 266 hr^{-1}. Compared with previous efforts relying on the use of Pd/C and Ru/C, which required mineral acids (e.g., H_2SO_4) to enable the FA-mediated deoxygenative reduction of HMF,[19,20] Au^$Pd_{0.2}$/*t*-ZrO_2 exhibited a TOF of at least one order of magnitude greater than that of the reported catalysts under H_2-free reaction conditions. Furthermore, the catalyst was reused at least six times without an appreciable loss of activity (Figure S12), during which time the total turnover number approached 2,400; this value is significantly greater than those reported for previous state-of-the-art systems. Notably, significant morphological or compositional changes were not detected by TEM, inductively coupled plasma mass spectrometry, and XPS (Figure S13) after catalysis, demonstrating the stable performance of the catalyst as observed from the durability tests. To the best of our knowledge, this Au^Pd-FA-mediated catalytic process exhibits the best activity ever reported for the targeted conversion of HMF to DMF.

Catalyst Development for DMF to PX

After demonstrating the complete capability of Au^$Pd_{0.2}$/*t*-ZrO_2 to enable a facile H_2-free HMF-to-DMF conversion, the feasibility of implementing the second step for making PX from HMF was assessed using the same catalytic material. In this regard, notably, most of the relevant studies carried out thus far for the dehydrative aromatization reaction using various zeolite-based solid acid catalysts[40–47] have reported an unacceptable product loss and undesirable rapid catalyst deactivation, related to the prevalence of uncontrolled overalkylation and/or oligomerization pathways triggered by the strong acidic Brönsted sites associated with the zeolitic frameworks. As such, we were particularly intrigued by the potential use of simple oxides such as ZrO_2 and related materials as alternative catalysts for this challenging transformation. Our initial studies dealing with the dehydrative aromatization of DMF with 4 MPa of ethylene in *n*-heptane at 250°C for 6 hr were promising and suggested that the oxide-assisted dehydrative aromatization is possible. Figure 2 summarizes the tests of several ubiquitous metal oxides. The results revealed that ZrO_2 polymorphs are particularly effective materials, with

Please cite this article in press as: Tao et al., Toward an Integrated Conversion of 5-Hydroxymethylfurfural and Ethylene for the Production of Renewable *p*-Xylene, Chem (2018), https://doi.org/10.1016/j.chempr.2018.07.007

Table 2. Dehydrative Aromatization of DMF into PX over Different Catalysts under Various Reaction Conditions

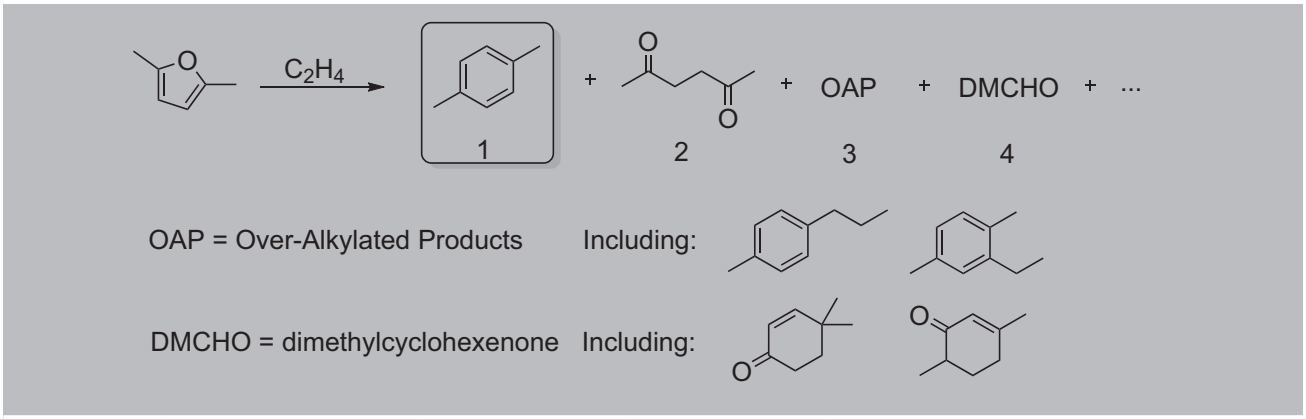

Entry	Catalyst	Temp. (°C)	Conv. (%)	Selectivity (%)			
				1	2	3	4
1	*t*-ZrO_2	250	41	95	–	<1	–
2	*t*-ZrO_2	275	56	93	–	2	–
3	*t*-ZrO_2	300	64	85	–	6	–
4[a]	*t*-ZrO_2	275	>99	90	–	3	–
5	Au^$Pd_{0.2}$/*t*-ZrO_2	275	51	93	–	2	–
6[a]	Au^$Pd_{0.2}$/*t*-ZrO_2	275	>99	88	–	3	–

Reaction conditions: 1 mmol DMF, 4 MPa ethylene, 5 mL *n*-heptane, 300 mg catalyst, 6 hr.
[a]Reaction time: 18 hr.

t-ZrO_2 exhibiting an outstanding selectivity for PX and excellent catalytic efficiency in the reaction.

In this case, 41% of DMF was converted to PX (39% gas chromatography yield), with a high selectivity of 95% (Table 2, entry 1). With further optimization, an excellent yield of PX (90%) was obtained after 18 hr by performing the reaction at 275°C (entry 4). Concerning the catalytic behavior of the different oxide-based samples, the data in Table S8 clearly show that there is a marked influence of the type and concentration of the surface acid sites on the performance of these oxide-based materials. It seems that the absence of low Brönsted acidity (in the case of SiO_2 or a TiO_2 sample as catalyst) or high population of Brönsted acid sites with moderate to strong acid strengths (as for Nb_2O_5, WO_3, and Al_2O_3) is detrimental for the PX formation. In fact, the main characteristics of the most effective single-phase ZrO_2-based materials, in particular, the *t*-ZrO_2 sample in its tetragonal crystal structure, is the presence of a high density of weak Lewis acid sites and a small amount of weak Brönsted acid sites, suggesting that the cooperative interaction between the weakly acidic Lewis and Brönsted acid sites is crucial in achieving optimal outcomes for making PX from DMF. More importantly, it is worth noting that this *t*-ZrO_2-based material is fully recoverable and reusable for at least five successive runs (Figure S14), a significant advantage over previous approaches based on zeolite catalysis.

t-ZrO_2-based oxides clearly show significant potential as a new class of efficient and effective solid acid catalysts for the highly selective transformation of DMF into PX. An important issue when dealing with *t*-ZrO_2-based nanocrystalline materials is their tetragonal-to-monoclinic phase transformation in the presence of water or water vapor even at relatively low temperature.[48] It is worthwhile to point out here that although water is one of the reaction products during the dehydrative conversion

Please cite this article in press as: Tao et al., Toward an Integrated Conversion of 5-Hydroxymethylfurfural and Ethylene for the Production of Renewable *p*-Xylene, Chem (2018), https://doi.org/10.1016/j.chempr.2018.07.007

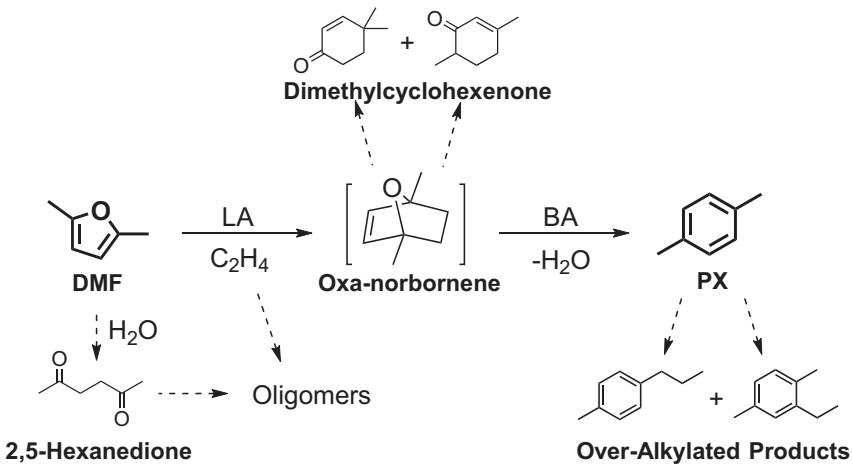

Scheme 2. Reaction Network of Dehydrative Aromatization of DMF with Ethylene

of DMF to PX (see Scheme 2), we do not observe any sort of polymorphic phase transformation of *t*-ZrO_2. In fact, no phases other than tetragonal zirconia could be identified by using X-ray diffraction to assess the phase purity of the spent samples (Figure S15). This serves as a strong indication that the *t*-ZrO_2 material is indeed stable during the present DMF-to-PX process. Although somewhat unexpected, it is important to further note that all these findings are also compatible with the results concerning textural measurements based on low-temperature nitrogen adsorption analysis, which did not show obvious changes in the Brunauer-Emmett-Teller (BET) specific surface areas, pore volumes, and average pore diameters of *t*-ZrO_2 after five successive runs (Figure S16). We envisioned that the very hydrophobic nature of the present reaction medium plays a key role in inhibiting the water-induced phase transformation of *t*-ZrO_2, although the exact reason for the enhanced phase stability remains to be clarified.

To put the catalytic performance of *t*-ZrO_2 into context, we also carried out the DMF-to-PX reaction under the optimal conditions using Brönsted acidic H-BEA and P-BEA, as well as Lewis acidic Sn-BEA zeolites, as reference materials at a substrate-to-acid molar ratio of 23 (consistent with 300 mg of *t*-ZrO_2). The results obtained (see Table S9) for the transformation of DMF show that the zeolite-based catalysts were, under the above conditions, far more active than *t*-ZrO_2, exhibiting an initial conversion rate of 7.82 $mol_{DMF}\cdot(h\cdot mol_{total\ acid\ sites})^{-1}$ compared with 2.38 $mol_{DMF}\cdot(h\cdot mol_{total\ acid\ sites})^{-1}$ measured for *t*-ZrO_2. As a result of the inherently lower selectivity associated with zeolite-based systems, however, the specific PX formation rate obtained for *t*-ZrO_2 is still favorably comparable with those of these zeolite-based materials. It is further noteworthy that, without post-calcination treatment in air at 500°C, these zeolite-based catalysts suffered from severe deactivation during a subsequent test run under otherwise identical conditions (Figure S17). A plausible explanation for the superior durability of *t*-ZrO_2 may lie in the fact that 2,5-hexanedione (an unwanted by-product resulting from H_2O-induced DMF ring opening, Scheme 2), being responsible for the notorious oligomerization-induced carbon loss commonly occurring on zeolite catalysts, can be essentially eliminated in such a non-zeolite-based system, which we confirmed in a separate experiment (Table S10).

An additional aspect that deserves attention is the capability of *t*-ZrO_2 to suppress the ethylene oligomerization pathway. Although largely ignored in the context of

Please cite this article in press as: Tao et al., Toward an Integrated Conversion of 5-Hydroxymethylfurfural and Ethylene for the Production of Renewable *p*-Xylene, Chem (2018), https://doi.org/10.1016/j.chempr.2018.07.007

DMF-to-PX transformations, catalytic ethylene oligomerization represents a topic of considerable current academic and industrial interest,[49] in particular for the production of linear α-olefins (LAOs) in the C_4–C_{10} range. It is pertinent to mention here that, as a result of a high tendency for coke formation triggered by zeolitic Brönsted acidic sites,[50] zeolite-catalyzed ethylene oligomerization is generally not selective for LAOs. To examine whether ethylene oligomerization on its own might occur as a minor side reaction, we performed additional experiments in which ethylene was employed as the sole reactant. It is noteworthy that although none of the samples tested yield any detectable amount of oligomer products, all of the zeolite-based materials turned from white to dark-brown after the reaction (Figure S18). TGA mass loss above 250°C for the ethanol-washed catalyst from the sole ethylene reactions catalyzed by H-BEA correspond to ca. 4 wt % of the initial ethylene mass (Figure S19). This finding contrasts with observations of the *t*-ZrO_2 material, which retains its white color, suggesting the absence of any oligomerization on this catalyst, as corroborated by a negligible TGA mass loss in this sample. Taken together, these findings underscored the central role of *t*-ZrO_2 in facilitating ultraselective PX formation in terms of full feedstock utilization by practically eliminating any unwanted pathways.

Although the mechanism for PX formation from DMF and ethylene is very complex and several key aspects regarding the role and relevance of surface acidity are still under debate,[51,52] the distinguished ability of *t*-ZrO_2 from those of zeolite-based materials could be attributed to its unique capability of controlling the reaction pathway through cooperation between weakly acidic Lewis and Brönsted acid sites. The involvement of both Lewis and Brönsted acid sites on *t*-ZrO_2 for dehydrative aromatization was well supported by the negative effects of titration with 2,6-lutidine or pyridine (Figure S20).[53,54] A major interest arising, then, is how the synergy between such Lewis and Brönsted acidity could facilitate this *t*-ZrO_2-mediated catalysis. Given that the Brönsted acid sites of *t*-ZrO_2 originate essentially from the hydroxyl-attached Zr species,[55] a more thoroughly dehydrated sample (denoted as *t*-ZrO_2-DH) was prepared and tested under the same conditions as the data in Table S11. As revealed by pyridine-infrared (IR) analysis (Figure S21), a prolonged post-calcination of as-prepared *t*-ZrO_2 at 400°C for 10 hr leads to an effective removal of Brönsted hydroxyls while retaining its Lewis acidity. This dehydrated material exhibited much lower PX yield compared with *t*-ZrO_2, which underlines the central role played by the Brönsted Zr-hydroxyls in determining the final performance of the *t*-ZrO_2-based materials. Meanwhile, by subjecting as-prepared *t*-ZrO_2 to a surface sulfation treatment, we were able to introduce additional strong Brönsted acidity in this material. The poor activity of this sample excludes the possibility of performance enhancement by the synergistic interactions between strong Brönsted acidity and the inherent Lewis acidity in the *t*-ZrO_2-based material.

To further understand how the surface Lewis acidity affects the Brönsted/Lewis cooperativity in *t*-ZrO_2, we prepared two additional control samples doped with low levels of aluminum and lanthanum, wherein we opted for a simple alcothermal approach for metal doping in zirconia. In such a way, Al and La cations could be introduced onto the *t*-ZrO_2 surface as extra Lewis acid sites to individually modulate the nature of surface Lewis acidity,[56,57] as supported by pyridine-IR and NH_3-TPD measurements (Figures S21 and S22; Table S12). We were thus able to establish that despite their similar weak surface Brönsted acidity, the amounts and strengths of Lewis acid decrease in the following order: *t*-ZrO_2-Al > *t*-ZrO_2 > *t*-ZrO_2-La. Notably, both doped samples displayed much inferior performance than that of *t*-ZrO_2 (Table S11). Because DMF to PX is a multistep reaction requiring specific functional sites for

Please cite this article in press as: Tao et al., Toward an Integrated Conversion of 5-Hydroxymethylfurfural and Ethylene for the Production of Renewable *p*-Xylene, Chem (2018), https://doi.org/10.1016/j.chempr.2018.07.007

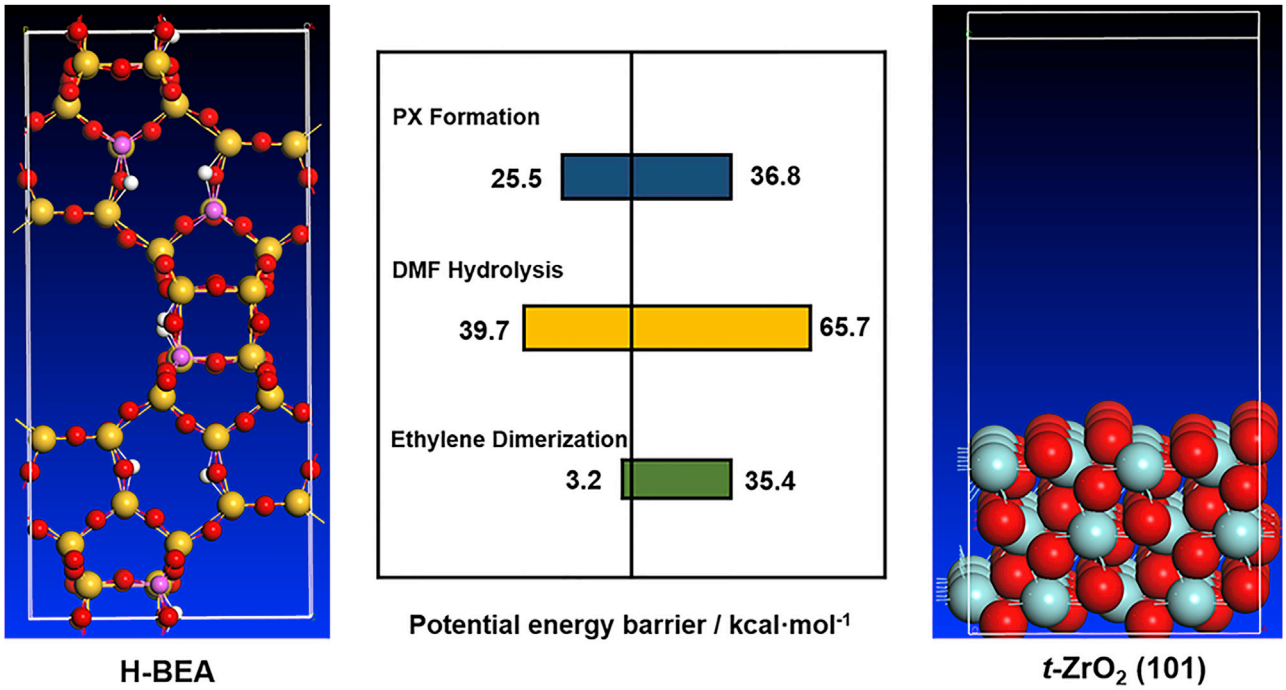

Figure 3. Overall Potential-Energy Barriers for the Dimerization of Ethylene, the Hydrolysis of DMF, and the Dehydrative Aromatization of DMF into PX over H-BEA and *t*-ZrO_2(101)

individual steps in the reaction (Scheme 2), a delicate interplay between different associated reaction pathways is a key issue for the high selectivity of PX. This is presumably ensured by the unique balance of Lewis-Brönsted acid pairs inherent to *t*-ZrO_2. With a close contact between the adjacent Lewis-Brönsted acid pairs, the transient oxanorbornene intermediate has a higher chance to undergo subsequent dehydration to produce PX rather than degrade as unwanted by-products. In agreement with this notion are the data from reaction profile analysis (Figure S23), which revealed an extremely low level of related side-product formation throughout the reaction over the undoped *t*-ZrO_2 sample. Taken together, the beneficial cooperation effects arising from the close proximity of weakly Brönsted and Lewis acid sites in *t*-ZrO_2 seem to play a key role in ensuring that the reaction proceeds in an ideal manner.

The density functional theory (DFT) calculations carried out on the *t*-ZrO_2(101) surface and an H-BEA zeolite model (Figure S24) have provided deeper molecular insights into the key aspects of the moderately acidic Lewis and Brönsted acid sites for pathway regulation (Figure 3). On the catalyst surface there are three competing reaction routes: the oligomerization of ethylene, the hydrolysis of DMF, and the Diels-Alder addition of ethylene to DMF to oxanorbornene and its subsequent tandem transformation to PX. To keep the oligomerization problem computationally tractable, we adopted the dimerization of ethylene as the probe for the oligomerization reaction. The DFT calculation results indicate that the dimerization of ethylene and the hydrolysis of DMF are much easier in the porous channels of H-BEA than those on the *t*-ZrO_2(101) surface (Figures S25 and S26). On the *t*-ZrO_2(101) surface, the energy barrier ($\Delta E_e^{\neq}$) for the first step of ethylene dimerization is 35.4 kcal·mol^{-1}, whereas it is just 3.2 kcal·mol^{-1} in H-BEA. On the *t*-ZrO_2(101) surface, the $\Delta E_e^{\neq}$ for the first step of the hydrolysis of DMF is 65.7 kcal·mol^{-1}, whereas

Please cite this article in press as: Tao et al., Toward an Integrated Conversion of 5-Hydroxymethylfurfural and Ethylene for the Production of Renewable *p*-Xylene, Chem (2018), https://doi.org/10.1016/j.chempr.2018.07.007

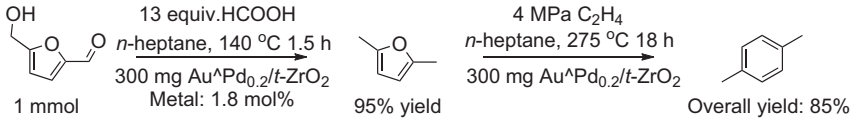

Scheme 3. One-Pot Two-Step Synthesis of PX Starting from HMF

it is just 39.7 kcal·mol^{-1} in H-BEA. On the other hand, the $\Delta E_e^{\neq}$ for the first step of the PX formation from DMF and ethylene is just 16.0 kcal·mol^{-1} on the *t*-ZrO_2(101) surface, whereas it is 16.8 kcal·mol^{-1} in H-BEA (Figure S27). Therefore, on the *t*-ZrO_2(101) surface, ethylene and DMF prefer to react with each other, whereas in the porous channels of H-BEA they prefer to oligomerize or hydrolyze. This is the reason that *t*-ZrO_2 is superior to H-BEA in the transformation of ethylene and DMF to PX.

The DFT calculation results also indicate that the synergistic effect between the Lewis and Brönsted acid sites plays a key role in the conversion of DMF to PX on the *t*-ZrO_2(101) surface (Figure S27). There are two key elementary steps for the formation of PX from ethylene and DMF on the *t*-ZrO_2(101) surface: the breaking of the C-O bond of the oxanorbornene intermediate and the dehydrogenation of a radical intermediate (IM5_Zr; Figure S30) to form PX. The DFT calculation results indicate that the active site for the breaking of the C-O bond of oxanorbornene is the Lewis acid site, whereas that for the formation of PX from IM5_Zr is the Brönsted acid site. On the Brönsted acid site, the $\Delta E_e^{\neq}$ for the breaking of the C-O bond of oxanorbornene is 23.6 kcal·mol^{-1}, whereas it is just 16.0 kcal·mol^{-1} on the Lewis acid site. For the formation of PX from IM5_Zr, the $\Delta E_e^{\neq}$ for this step is 20.2 kcal·mol^{-1} on the Brönsted acid site whereas it is 36.1 kcal·mol^{-1} without the help of the Brönsted acid site. It can be seen that both the Lewis and Brönsted acid sites are important for the conversion. Therefore, the activity and selectivity of the catalyst can be tuned by changing the ratio and density of the two types of sites.

Process Development for HMF to PX

Given these findings, we were particularly interested in examining whether Au^$Pd_{0.2}$/*t*-ZrO_2 could also exhibit excellent performance for the synthesis of PX from DMF. Much to our delight the reaction between DMF and ethylene was barely affected by the presence of additional Au-Pd species in the *t*-ZrO_2 system (Table 2, entries 5 and 6). This indicates that while the role of the metals is to catalyze the reductive reaction step to yield DMF, the dehydrative aromatization reaction is carried out by the underlying support, i.e., *t*-ZrO_2, and thus is virtually independent of the metals used. Hence, a two-stage, one-pot process is developed in which Au^$Pd_{0.2}$/*t*-ZrO_2 affects H_2-free hydrogenolysis, and the underlying *t*-ZrO_2 support then promotes the dehydrative aromatization to obtain PX from HMF. In addition, the possibility of coupling these two reactions in a single-pot process to directly produce PX from HMF was explored. This is by far the most relevant solution for the future production of PX from a sustainable viewpoint. To this end, HMF was first transformed into DMF with FA in *n*-heptane over the Au^$Pd_{0.2}$/*t*-ZrO_2 catalyst, and after flushing out the H_2-CO_2 mixtures generated *in situ*, 4 MPa of ethylene was introduced into the reaction system (Scheme 3).[58] The results indicated that a high HMF conversion with excellent selectivity for PX can be achieved by this one-pot procedure. Taken together, these findings indicate that a single catalyst-mediated direct synthesis of PX from HMF is achievable.

Please cite this article in press as: Tao et al., Toward an Integrated Conversion of 5-Hydroxymethylfurfural and Ethylene for the Production of Renewable *p*-Xylene, Chem (2018), https://doi.org/10.1016/j.chempr.2018.07.007

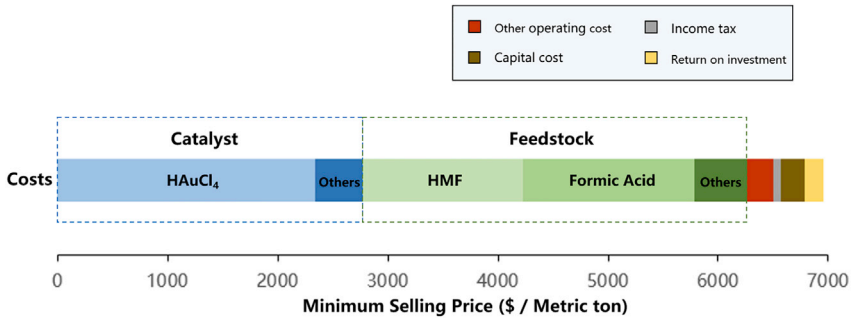

Figure 4. Techno-Economic Analysis of the Production of PX from HMF
For detailed cost distribution, see Table S17.

Examining the above data from a techno-economic perspective leads to identification of key process parameters that have to be greatly improved to promote future development of this PX-targeted technology. A detailed description of the process, the assumptions made, and the model used are available in the Supplemental Information. On the basis of the process model as depicted in Figure S31, our proposed integrated approach can produce PX at a minimum selling price (MSP) of $6,958 per metric ton (Figure 4). This unduly high level of MSP can be mainly attributed to the high HMF and FA feedstock costs, as well as the high cost arising from catalyst manufacturing, which has been identified as the major contributor to the overall process costs. From a practical perspective, future research should focus on a full optimization of the reaction parameters and further development of fully non-noble metal-based catalyst systems for the selective production of PX by means of the highly integrated conversion of HMF. While advances in the FA utilization efficiency as well as the TOF of PX production are necessary steps toward establishing a practically viable process, we anticipate that significant improvements in these areas will also benefit from the continuously improved biorefinery supply chains, which would lead to strongly reduced feedstock costs.

DISCUSSION

In summary, we demonstrated for the first time a highly effective protocol for the direct synthesis of PX from HMF through a two-stage, one-pot procedure mediated by a single catalyst. With characteristics such as energy savings and no additional separation steps or catalysts, our method represents a rare example of an integrated approach for target-specific conversion of bio-based multicomponent feedstocks into renewable industrial products in a highly efficient and effective manner, which is difficult to achieve using other catalytic systems. These findings clearly demonstrate the great potential for multiscale design in achieving new one-pot multistep transformations as a compelling strategy that can unlock the potential of bio-renewable resources as feedstocks to produce industrially important commodity chemicals.

EXPERIMENTAL PROCEDURES

Preparation of Au/*t*-ZrO_2

Au/*t*-ZrO_2 catalysts were prepared by a modified deposition-precipitation method by mixing *t*-ZrO_2 powders (1 g) with aqueous solutions of appropriate amounts of chloroauric acid (100 mL). The pH was then adjusted to 9.0 by dropwise addition of 0.25 M $NH_3 \cdot H_2O$. After 6 hr of stirring at 25°C the catalyst was washed five times with deionized water and separated by filtration. The samples were dried under vacuum at 25°C for 12 hr, followed by reduction with a stream of 5 vol % H_2/Ar

at 300°C for 2 hr. The BET surface area of the resultant Au/*t*-ZrO_2 catalyst was 105 $m^2 \cdot g^{-1}$.

Preparation of Au^Pd_x/*t*-ZrO_2

Au^Pd_x/*t*-ZrO_2 catalysts were prepared by a wet chemical reduction method. Typically, 300 mg of Au/*t*-ZrO_2 catalyst was introduced into aqueous solutions of appropriate amounts of palladium chloride (5 mL). The solution was then stirred at 25°C for 10 min followed by the addition of aqueous solutions of appropriate amounts of sodium borohydride (5 mL). After 30 min of stirring at 25°C the catalyst was washed five times with deionized water and separated by filtration. The samples were dried under vacuum at 25°C for 12 hr followed by reduction with a stream of 5 vol % H_2/Ar at 300°C for 0.5 hr before use.

General Procedure for FA-Mediated Catalytic Conversion of HMF into DMF

A mixture of HMF (2 mmol), FA (designated amount), catalysts (designated amount), 1,4-dioxane (5 mL), and dodecane (1 mmol, as the internal standard) were charged into a 50-mL Hastelloy-C high-pressure Parr reactor. The resulting mixture was vigorously stirred (800 rpm) under a N_2 atmosphere (1 atm) at the designed temperature for the given reaction time. After completion of the reaction, the reaction mixture was filtered and the catalyst was washed thoroughly with ethanol. The filtrate was then collected and analyzed by an Agilent 7820A gas chromatograph equipped with an HP-INNOWax column (30 m × 0.32 mm × 0.25 μm) and a flame ionization detector (FID). All of the products were identified by gas chromatography-mass spectrometry (GC-MS), and the spectra obtained were compared with the standard spectra.

General Procedure for Dehydrative Aromatization of DMF into PX

A mixture of DMF (1 mmol), catalysts (designated amount), *n*-heptane (5 mL), and naphthalene (1 mmol, as the internal standard) were charged into a 50-mL Hastelloy-C high-pressure Parr reactor. The resulting mixture was vigorously stirred (800 rpm) under an ethylene atmosphere (40 atm) at the designated temperature for the given reaction time. After completion of the reaction, the reaction mixture was filtered and the catalyst was washed thoroughly with ethanol. The filtrate was then collected and analyzed by an Agilent 7820A gas chromatograph equipped with an HP-INNOWax column (30 m × 0.32 mm × 0.25 μm) and an FID. All of the products were identified by GC-MS, and the spectra obtained were compared with the standard spectra.

Recovery and Reuse of Catalysts

The catalyst was collected after filtration, and washed with ethanol three times and then with distilled water several times. The catalyst was then dried under vacuum at 25°C for 12 hr before being used for the next reaction.

SUPPLEMENTAL INFORMATION

Supplemental Information includes Supplemental Experimental Procedures, 32 figures, and 17 tables and can be found with this article online at https://doi.org/10.1016/j.chempr.2018.07.007.

ACKNOWLEDGMENTS

This work was supported by National Natural Science Foundation of China (21473035, 91545108, 21773033, 91645201), Science & Technology Commission of Shanghai Municipality (16ZR1440-400), SINOPEC (X514005), and the Open Project of State Key Laboratory of Chemical Engineering (SKL-ChE-15C02). We also

thank Zhongtian Mao from University of Washington, Seattle for assistance with data analysis.

AUTHOR CONTRIBUTIONS

Y.C. and L.T. conceived the idea and designed the experiments. L.T. and T.-H.Y. performed the preparation and characterization of catalysts. L.T., T.-H.Y., Y.Z., and Q.Z. performed the experiments and analyzed the results. W.L. and M.M.W. did the techno-economic analysis. Z.-H.L. carried out the DFT calculations. H.-Y.H. advised on paper writing. L.T., Y.-M.L., and Y.C. supervised the project and co-wrote the paper. All authors discussed the results and commented on the manuscript.

DECLARATION OF INTERESTS

The authors declare no competing interests.

Received: March 13, 2018
Revised: June 19, 2018
Accepted: July 12, 2018
Published: August 9, 2018

REFERENCES AND NOTES

1. Van Uytyanck, P.P., Haire, G., and Dennis, J.S. (2017). Impact on the polyester value chain of using p-xylene derived from biomass. ACS Sustain. Chem. Eng. *5*, 4119–4126.

2. Grand View Research. (2016). Para-xylene market analysis by application (dimethyl terephthalate (DMT), purified terephthalic acid (PTA)) and segment forecasts to 2022. https://www.grandviewresearch.com/industry-analysis/paraxy-lene-market. Accessed on 6th June 2018.

3. Sholl, D.S., and Lively, R.P. (2016). Seven chemical separations to change the world. Nature *532*, 435–437.

4. Aronen, S. (2013). Aromatics processing made safe and efficient with proper valve selection. https://www.metso.com/showroom/oil-and-gas/aromatics-proce-ssing-made-safe-and-efficient-with-proper-valve-selection. Accessed on 6th June 2018. Note that as an essential part of the chemical industry, the BTX aromatics are produced globally with total volume of approx. 110 million metric tons per year.

5. Cavani, F., Albonetti, S., and Basile, F. (2016). Chapter 2. Aromatics from biomasses: technological options for chemocatalytic transformations. In Chemicals and Fuels from Bio-based Building Blocks, F. Cavani, S. Albonetti, F. Basile, and A. Gandini, eds. (Wiley-VCH), pp. 33–50.

6. Settle, A.E., Bertis, L., Rorrer, N.A., Roman-Leshkóv, Y., Beckham, G.T., Richards, R.M., and Vardon, D.R. (2017). Heterogeneous Diels-Alder catalysis for biomass-derived aromatic compounds. Green Chem. *19*, 3468–3492.

7. Saha, B., and Abu-Omar, M.M. (2015). Current technologies, economics, and perspectives for 2,5-dimethylfuran production from biomass-derived intermediates. ChemSusChem *8*, 1133–1142.

8. Maneffa, A., Priecel, P., and Lopez-Sanchez, J.A. (2016). Biomass-derived renewable aromatics: selective routes and outlook for p-xylene commercialisation. ChemSusChem *9*, 2736–2748.

9. Lyons, T.W., Guironnet, D., Findlater, M., and Brookhart, M. (2012). Synthesis of p-xylene from ethylene. J. Am. Chem. Soc. *134*, 15708–15711.

10. Sun, J., Liu, C., Wang, Y., Smith, C., Martin, K., and Venkitasubramanian, P. (2014). US20140121430A1.

11. Peters, M.W., Taylor, J.D., Jenni, M., Manzer, L.E., and Henton, D.E. (2011). US20110087000.

12. Dutta, S., De, S., Alam, M.I., Abu-Omar, M.M., and Saha, B. (2012). Direct conversion of cellulose and lignocellulosic biomass into chemicals and biofuel with metal chloride catalysts. J. Catal. *288*, 8–15.

13. Wang, T., Nolte, M.W., and Shanks, B.H. (2014). Catalytic dehydration of C_6 carbohydrates for the production of hydroxymethylfurfural (HMF) as a versatile platform chemical. Green Chem. *16*, 548–572.

14. Cai, C.M., Nagane, N., Kumar, R., and Wyman, C.E. (2014). Coupling metal halides with a co-solvent to produce furfural and 5-HMF at high yields directly from lignocellulosic biomass as an integrated biofuels strategy. Green Chem. *16*, 3819–3829.

15. Mirzaei, H.M., and Karimi, B. (2016). Sulphanilic acid as a recyclable bifunctional organocatalyst in the selective conversion of lignocellulosic biomass to 5-HMF. Green Chem. *18*, 2282–2286.

16. Binder, J.B., and Raines, R.T. (2009). Simple chemical transformation of lignocellulosic biomass into furans for fuels and chemicals. J. Am. Chem. Soc. *131*, 1979–1985.

17. Teixeira, I.F., Lo, B.T.W., Kostetskyy, P., Stamatakis, M., Ye, L., Tang, C.C., Mpourmpakis, G., and Tsang, S.C.E. (2016). From biomass-derived furans to aromatics with ethanol over zeolite. Angew. Chem. Int. Ed. *55*, 13061–13066.

18. Wang, D., Osmundsen, C.M., Taaming, E., and Dumesic, J.A. (2013). Selective production of aromatics from alkylfurans over solid acid catalysts. ChemCatChem *5*, 2044–2050.

19. De, S., Dutta, S., and Saha, B. (2012). One-pot conversions of lignocellulosic and algal biomass into liquid fuels. ChemSusChem *5*, 1826–1833.

20. Thananatthanachon, T., and Rauchfuss, T.B. (2010). Efficient production of the liquid fuel 2,5-dimethylfuran from fructose using formic acid as a reagent. Angew. Chem. Int. Ed. *49*, 6616–6618.

21. Yang, P., Xia, Q., Liu, X., and Wang, Y. (2017). Catalytic transfer hydrogenation/hydrogenolysis of 5-hydroxymethylfurfural to 2,5-dimethylfuran over Ni-Co/C catalyst. Fuel *187*, 159–166.

22. Jae, J., Zheng, W., Karim, A.M., Guo, W., Lobo, R.F., and Vlachos, D.G. (2014). The role of Ru and RuO_2 in the catalytic transfer hydrogenation of 5-hydroxymethylfurfural for the production of 2,5-dimethylfuran. ChemCatChem *6*, 848–856.

23. Scholz, D., Aellig, C., and Hermans, I. (2013). Catalytic transfer hydrogenation/hydrogenolysis for reductive upgrading of furfural and 5-(hydroxymethyl)furfural. ChemSusChem *7*, 268–275.

24. Jae, J., Zheng, W., Lobo, R.F., and Vlachos, D.G. (2013). Production of dimethylfuran from hydroxymethylfurfural through catalytic transfer hydrogenation with ruthenium supported on carbon. ChemSusChem *6*, 1158–1162.

25. Du, X.L., He, L., Zhao, S., Liu, Y.M., Cao, Y., He, H.Y., and Fan, K.N. (2011). Hydrogen-independent reductive transformation of carbohydrate biomass into γ-valerolactone and pyrrolidone derivatives with supported gold catalysts. Angew. Chem. Int. Ed. *50*, 7815–7819.

26. Yuan, J., Li, S.S., Yu, L., Liu, Y.M., Cao, Y., He, H.Y., and Fan, K.N. (2013). Copper-based catalysts for the efficient conversion of carbohydrate biomass into γ-valerolactone in the absence of externally added hydrogen. Energy Environ. Sci. *6*, 3308–3313.

27. Bi, Q.Y., Lin, J.D., Liu, Y.M., He, H.Y., Huang, F.Q., and Cao, Y. (2016). Dehydrogenation of formic acid at room temperature: boosting palladium nanoparticle efficiency by coupling with pyridinic-nitrogen-doped carbon. Angew. Chem. Int. Ed. *55*, 11849–11853.

28. Bi, Q.Y., Lin, J.D., Liu, Y.M., Du, X.L., He, H.Y., and Cao, Y. (2014). An aqueous rechargeable formate-based hydrogen battery driven by heterogeneous Pd catalysis. Angew. Chem. Int. Ed. *53*, 13583–13587.

29. Bi, Q.Y., Du, X.L., Liu, Y.M., Cao, Y., He, H.Y., and Fan, K.N. (2012). Efficient subnanometric gold-catalyzed hydrogen generation via formic acid decomposition under ambient conditions. J. Am. Chem. Soc. *134*, 8926–8933.

30. Li, S.S., Tao, L., Wang, F.Z.R., Liu, Y.M., and Cao, Y. (2016). Heterogeneous gold-catalyzed selective semireduction of alkynes using formic acid as hydrogen source. Adv. Synth. Catal. *358*, 1410–1416.

31. Yu, L., Zhang, Q., Li, S.S., Huang, J., Liu, Y.M., He, H.Y., and Cao, Y. (2015). Gold-catalyzed reductive transformation of nitro compounds using formic acid: mild, efficient, and versatile. ChemSusChem *8*, 3029–3035.

32. Tao, L., Zhang, Q., Li, S.S., Liu, X., Liu, Y.M., and Cao, Y. (2015). Heterogeneous gold-catalyzed selective reductive transformation of quinolines with formic acid. Adv. Synth. Catal. *357*, 753–760.

33. Liu, X., Li, S.S., Liu, Y.M., and Cao, Y. (2015). Formic acid: a versatile renewable reagent for green and sustainable chemical synthesis. Chinese J. Catal. *36*, 1461–1475.

34. Mitra, J., Zhou, X., and Rauchfuss, T. (2015). Pd/C-catalyzed reactions of HMF: decarbonylation, hydrogenation, and hydrogenolysis. Green Chem. *17*, 307–313.

35. Dimitratos, N., Lopez-Sanchez, J.A., Morgan, D., Carley, A.F., Tiruvalam, R., Kiely, C.J., Bethella, D., and Hutchings, G.J. (2009). Solvent-free oxidation of benzyl alcohol using Au-Pd catalysts prepared by sol immobilisation. Phys. Chem. Chem. Phys. *11*, 5142–5153.

36. Pritchard, J., Kesavan, L., Piccinini, M., He, Q., Tiruvalam, R., Dimitratos, N., Lopez-Sanchez, J.A., Carley, A.F., Edwards, J.K., Kiely, C.J., and Hutchings, G.J. (2010). Direct synthesis of hydrogen peroxide and benzyl alcohol oxidation using Au-Pd catalysts prepared by sol immobilization. Langmuir *26*, 16568–16577.

37. Kesavan, L., Tiruvalam, R., Ab Rahim, M.H., bin Saiman, M.I., Enache, D.I., Jenkins, R.L., Dimitratos, N., Lopez-Sanchez, J.A., Taylor, S.H., Knight, D.W., et al. (2011). Solvent-free oxidation of primary carbon-hydrogen bonds in toluene using Au-Pd alloy nanoparticles. Science *331*, 195–199.

38. Chiorino, A., Manzoli, M., Menegazzo, F., Signoretto, M., Vindigni, F., Pinna, F., and Boccuzzi, F. (2009). New insight on the nature of catalytically active gold sites: quantitative CO chemisorption data and analysis of FTIR spectra of adsorbed CO and of isotopic mixtures. J. Catal. *262*, 169–176.

39. Pei, G.X., Liu, X.Y., Wang, A., Li, L., Huang, Y., Zhang, T., Lee, J.W., Jang, B.W.L., and Mou, C.Y. (2014). Promotional effect of Pd single atoms on Au nanoparticles supported on silica for the selective hydrogenation of acetylene in excess ethylene. New J. Chem. *38*, 2043–2051.

40. Williams, C.L., Chang, C.C., Do, P., Nikbin, N., Caratzoulas, S., Vlachos, D.G., Lobo, R.F., Fan, W., and Dauenhauer, P.J. (2012). Cycloaddition of biomass-derived furans for catalytic production of renewable p-xylene. ACS Catal. *2*, 935–939.

41. Chang, C.C., Green, S.K., Williams, C.L., Dauenhauer, P.J., and Fan, W. (2014). Ultra-selective cycloaddition of dimethylfuran for renewable p-xylene with H-BEA. Green Chem. *16*, 585–588.

42. Kim, T.W., Kim, S.Y., Kim, J.C., Kim, Y., Ryoo, R., and Kim, C.U. (2016). Selective p-xylene production from biomass-derived dimethylfuran and ethylene over zeolite beta nanosponge catalysts. Appl. Catal. B *185*, 100–109.

43. Cho, H.J., Ren, L., Vattipalli, V., Yeh, Y.H., Gould, N., Xu, B., Gorte, R.J., Lobo, R., Dauenhauer, P.J., Tsapatsis, M., and Fan, W. (2017). Renewable p-xylene from 2,5-dimethylfuran and ethylene using phosphorus-containing zeolite catalysts. ChemCatChem *9*, 398–402.

44. Wijaya, Y.P., Suh, D.J., and Jae, J. (2015). Production of renewable p-xylene from 2,5-dimethylfuran via Diels-Alder cycloaddition and dehydrative aromatization reactions over silica-alumina aerogel catalysts. Catal. Commun. *70*, 12–16.

45. Kim, J.C., Kim, T.W., Kim, Y., Ryoo, R., Jeong, S.Y., and Kim, C.U. (2017). Mesoporous MFI zeolites as high performance catalysts for Diels-Alder cycloaddition of bio-derived dimethylfuran and ethylene to renewable p-xylene. Appl. Catal. B *206*, 490–500.

46. Yu, J., Zhu, S., Dauenhauer, P.J., Cho, H.J., Fan, W., and Gorte, R.J. (2016). Adsorption and reaction properties of SnBEA, ZrBEA and H-BEA for the formation of p-xylene from DMF and ethylene. Catal. Sci. Technol. *6*, 5729–5736.

47. Pacheco, J.J., Labinger, J.A., Sessions, A.L., and Davis, M.E. (2015). Route to renewable PET: reaction pathways and energetics of Diels-Alder and dehydrative aromatization reactions between ethylene and biomass-derived furans catalyzed by Lewis acid molecular sieves. ACS Catal. *5*, 5904–5913.

48. Xie, S., Iglesia, E., and Bell, A.T. (2000). Water-assisted tetragonal-to-monoclinic phase transformation of ZrO_2 at low temperatures. Chem. Mater. *12*, 2442–2447.

49. Speiser, F., Braunstein, P., and Saussine, L. (2005). Catalytic ethylene dimerization and oligomerization: recent developments with nickel complexes containing P,N-chelating ligands. Acc. Chem. Res. *38*, 784–793.

50. Díaz-Rey, M.R., Paris, C., Martínez-Franco, R., Moliner, M., Martínez, C., and Corma, A. (2017). Efficient oligomerization of pentene into liquid fuels on nanocrystalline beta zeolites. ACS Catal. *7*, 6170–6178.

51. Nikbin, N., Do, P.T., Caratzoulas, S., Lobo, R.F., Dauenhauer, P.J., and Vlachos, D.G. (2013). A DFT study of the acid-catalyzed conversion of 2,5-dimethylfuran and ethylene to p-xylene. J. Catal. *297*, 35–43.

52. Nikbin, N., Feng, S., Caratzoulas, S., and Vlachos, D.G. (2013). p-Xylene formation by dehydrative aromatization of a Diels-Alder product in Lewis and Brønsted acidic zeolites. J. Phys. Chem. C *118*, 24415–24424.

53. Yamaguchi, K., Kobayashi, H., Wang, Y., Oishi, T., Osasawara, Y., and Mizuno, N. (2013). Green oxidative synthesis of primary amides from primary alcohols or aldehydes catalyzed by a cryptomelane-type manganese oxide-based octahedral molecular sieve, OMS-2. Catal. Sci. Technol. *3*, 318–327.

54. Tao, L., Wang, Z.J., Yan, T.H., Liu, Y.M., He, H.Y., and Cao, Y. (2017). Direct synthesis of pyrroles via heterogeneous catalytic condensation of anilines with bioderived furans. ACS Catal. *7*, 959–964.

55. Arce-Ramos, J.M., Grabow, L.C., Handy, B.E., and Cárdenas-Galindo, M.G. (2015). Nature of acid sites in silica-supported zirconium oxide: a combined experimental and periodic DFT study. J. Phys. Chem. C *119*, 15150–15159.

56. Caillot, T., Salama, Z., Chanut, N., Cadete Santos Aires, F.J., Bennici, S., and Auroux, A. (2013). Hydrothermal synthesis and characterization of zirconia based catalysts. J. Solid State Chem. *203*, 79–85.

57. Lahousse, C., Aboulayt, A., Maugé, F., Bachelier, J., and Lavalley, J.C. (1993). Acidic and basic properties of zirconia-alumina and zirconia-titania mixed oxides. J. Mol. Catal. *84*, 283–297.

58. It is important to note that, based on an extensive solvent screening and assessment (see Table S13 for details), *n*-heptane was proven to be the most suitable solvent to implement a fully integrated process without compromising the conceptual integrity and the process performance at all stages of the overall process.